

Inflammatory Response Leads to Neuronal Death in Human Post-Mortem Cerebral Cortex in Patients with COVID-19

Mahdi Eskandarian Boroujeni,[●] Leila Simani,[●] Hans A. R. Bluysen, Hamid Reza Samadikhah, Soheila Zamanlui Benisi, Sanaz Hassani, Nader Akbari Dilmaghani, Mobina Fathi, Kimia Vakili, Gholam-Reza Mahmoudiasl, Hojjat Allah Abbaszadeh, Meysam Hassani Moghaddam, Mohammad-Amin Abdollahifar,^{*} and Abbas Aliaghaei^{*}

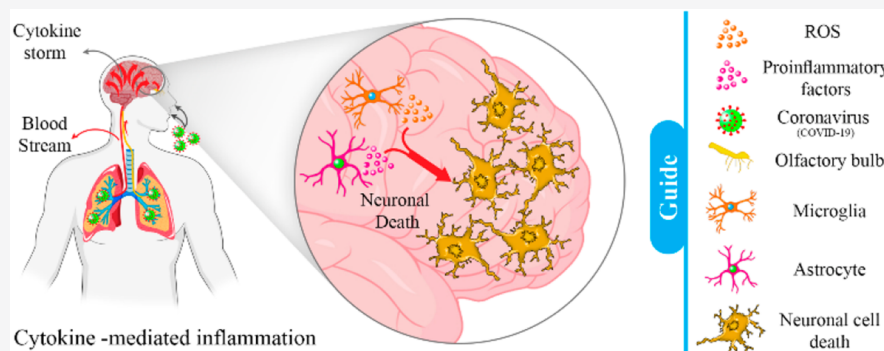
Cite This: *ACS Chem. Neurosci.* 2021, 12, 2143–2150

Read Online

ACCESS |

Metrics & More

Article Recommendations



ABSTRACT: The recent coronavirus disease of 2019 (COVID-19) pandemic has adversely affected people worldwide. A growing body of literature suggests the neurological complications and manifestations in response to COVID-19 infection. Herein, we explored the inflammatory and immune responses in the post-mortem cerebral cortex of patients with severe COVID-19. The participants comprised three patients diagnosed with severe COVID-19 from March 26, 2020, to April 17, 2020, and three control patients. Our findings demonstrated a surge in the number of reactive astrocytes and activated microglia, as well as low levels of glutathione along with the upregulation of inflammation- and immune-related genes IL1B, IL6, IFITM, MX1, and OAS2 in the COVID-19 group. Overall, the data imply that oxidative stress may invoke a glial-mediated neuroinflammation, which ultimately leads to neuronal cell death in the cerebral cortex of COVID-19 patients.

KEYWORDS: COVID-19, oxidative stress, neuroinflammation, cerebral cortex

INTRODUCTION

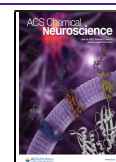
In December of 2019, a novel coronavirus called severe acute respiratory syndrome coronavirus 2 (SARS-CoV-2) emerged in Wuhan, China, causing the coronavirus disease of 2019 (COVID-19).¹ Although COVID-19 is primarily a respiratory virus, it may spread to nonrespiratory sites like the brain with associated neurological manifestations including smell and taste disturbances, headaches, vision impairment, and stroke.² The presence of COVID-19 in the brain has been shown by the detection of COVID-19 RNA in the cerebrospinal fluid (CSF) in patients with COVID-19.³ In addition, it is revealed that the spike 1 protein (S1) of COVID-19 can cross the murine blood–brain barrier (BBB) through the adsorptive transcytosis-mediated mechanism.⁴ However, the bulk of reports suggest that COVID-19 is not detectable in the CSF of patients with COVID-19 and neurological symptoms.⁵ Moreover, the post-mortem analysis of brain tissues from COVID-19 infected

individuals reveal inflammatory response-mediated blood vessel damage with no evidence of viral infection.⁶ It suggests that the virus cannot directly attack the brain in the infected patients. Herein, given the negative result of the COVID-19 test in the CSF of COVID-19 patients in this study, we sought to explore the impact of neuroinflammatory and antiviral responses combined with the oxidative stress that might play major roles in neuronal cell death in the cerebral cortex of patients with COVID-19.

Received: March 1, 2021

Accepted: May 25, 2021

Published: June 8, 2021



RESULTS AND DISCUSSION

COVID-19 Triggers a Reduction in the Number of Neuronal Cells and Changes the Spatial Arrangement of the Neurons in the Cerebral Cortex. The participants included three patients with severe COVID-19 and three age- and sex-matched control groups (Table 1). A hematoxylin and

Table 1. Demographic and Clinical Characteristics of Subjects in the Study Groups

variables	control	case	P value
sex			
male/female	3/0	2/1	0.273
age	35.33 ± 5.03	42.33 ± 7.50	0.251
RT-PCR for COVID-19	negative	positive	

eosin (H&E) staining of the cerebral cortex showed a decrease in the number of neurons in the brain of individuals infected by COVID-19 (Figure 1A,B; Supplementary Figure S1). Moreover,

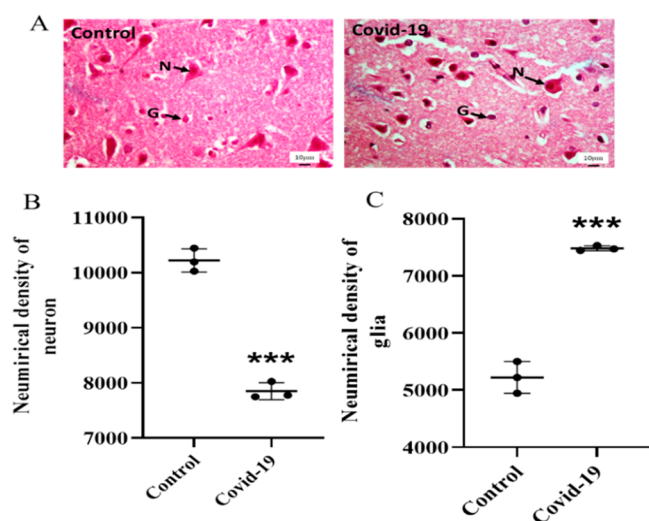


Figure 1. (A) H&E staining of the cerebral cortex. Black arrows show neurons (N) and glial cells (G) in control and COVID-19 groups. (B) The number of neurons decreased in COVID-19 patients compared to the control group (***) $P < 0.001$, while the number of glial cells remarkably increased in the COVID-19 group in comparison with the control (***) $P < 0.001$.

the brains from COVID-19 exhibited marked histological damages with increased infiltration and vasculitis (Figure 2). A Voronoi tessellation of the cerebral cortex neurons in the control and COVID-19 groups was performed (Figure 3A). The data revealed that 34.2% of the areas of the Voronoi polygons in the

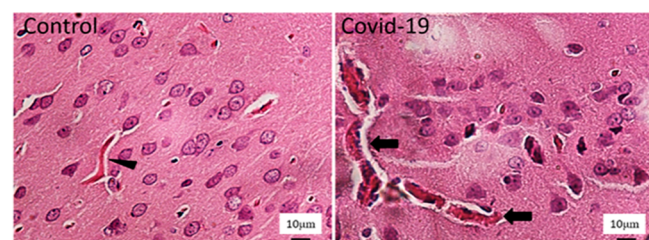


Figure 2. H&E-stained brain sections of the cerebral cortex in control and COVID-19 groups. Healthy vessel (arrowhead) and vasculitis (long arrow) are depicted.

cerebral cortex in the control group were in the range of less than or equal to $300 \mu\text{m}^2$. However, in COVID-19 only 11.11% of the polygon areas of the neurons were in this range. Besides, in the COVID-19 group, most of the polygon areas (27.77%) were in the range of $300\text{--}500 \mu\text{m}^2$ (Figure 3B). On the basis of the spatial distribution of neurons, the mean coefficient of variation (CV) of polygon areas in both groups was in a random range (33%–64%) (Figure 3C).

Herein, the neuronal loss in the cerebral cortex of the COVID-19 group was demonstrated by a reduction in the number of neurons and also substantial changes in the spatial arrangement of neurons. Moreover, the areas of the Voronoi polygons showed a variation in the COVID-19 infected group, indicating irregularities in the dendritic length due to cell death or an inflammatory process in the brain of these cases.

The Number of Glial Cells Is Increased in the Cerebral Cortex of COVID-19 Patients. The stereological analysis of the cerebral cortex also demonstrated a considerable surge in the number of glia cells in the cerebral cortex of individuals with COVID-19 (Figure 1A,C). Moreover, a cell count analysis by immunohistochemistry also showed elevated numbers of Iba-1-positive microglia cells and GFAP-positive astrocytes (both are glia cells) in the cerebral cortex samples of COVID-19 patients (Figure 4A–C).

Previous reports have indicated the possibility of the development of reactive astrogliosis in COVID-19 patients.⁷ For instance, Kangberg et al. revealed that the plasma concentration of the GFAP significantly increases in moderate to severe COVID-19 patients.⁸ In addition, Reichard et al. reported a generalized increase in GFAP expression in the white matter of a COVID-19 patient who had passed away due to disseminated encephalomyelitis.⁹

COVID-19 Causes Alterations in the Morphological Characteristics of Microglia Cells. To quantitatively investigate the morphology of microglial cells, a Sholl analysis was performed. Accordingly, COVID-19 infection remarkably reduced the morphological complexity of the microglia in terms of long branching processes (Figure 5A). Similarly, the examination of the length of the microglia processes unveiled that the process length of these cells had significantly decreased in the COVID-19 group (Figure 5B), indicating the presence of activated microglia with a reduced process length, which paves the way for the production of pro-inflammatory cytokines.¹⁰ Similarly, prior reports unveiled that activated microglia and reactive astrocytes are involved in the pathology of neurodegenerative disorders.¹¹ Thus, the elevated number of these cells can be associated with inflammation and brain tissue damage.

The Upregulation of Inflammation- and Immune-Related Genes and Low Glutathione Levels in the Cerebral Cortex of COVID-19 Patients. The expression level of interleukin 1 beta ($\text{IL-1}\beta$), interferon-inducible transmembrane (IFITM), MX dynamin-like GTPase 1 (MX1), interleukin 6 (IL-6), 2',5'-oligoadenylate synthetase 2 (OAS2), and angiotensin-converting enzyme 2 (ACE2) were assessed by real-time (RT) quantitative polymerase chain reaction (qPCR) (Figure 6). Accordingly, we observed the upregulation of inflammatory and immune-related genes $\text{IL-1}\beta$, IL-6, IFITM, MX1, and OAS2 in the COVID-19 group compared to the healthy individuals. However, the expression level of ACE2 showed no significant difference between COVID-19 and healthy groups.

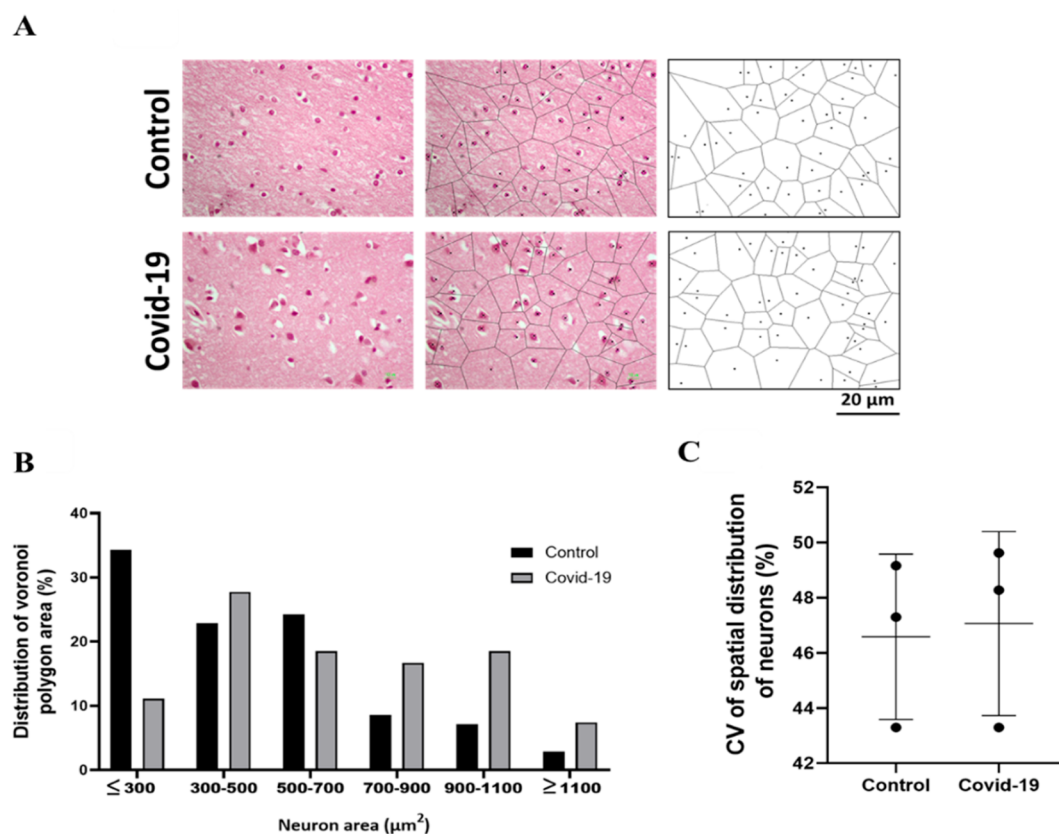


Figure 3. (A) A micrograph of neurons and a schematic of a Voronoi tessellation in the cerebral cortex in the control and COVID-19 groups. Each polygon represents the space that a cell occupies. (B) Distribution of Voronoi polygon area (%) and (C) CV of the spatial distribution of neurons in the cerebral cortex.

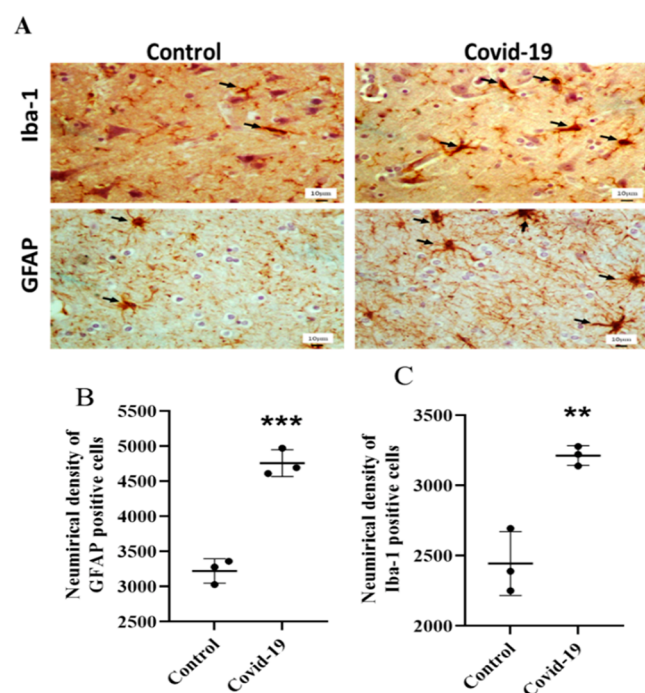


Figure 4. (A) Immunohistochemical staining against GFAP and Iba-1 was conducted in both COVID-19 and control groups. Black arrows represent GFAP positive astrocytes and Iba-1 positive microglia. (B, C) The number of astrocytes (***) and microglia (***) increased significantly in COVID-19 patients compared to the control.

Multiple lines of evidence have shown that both microglia and astrocytes are highly sensitive to the pro-inflammatory cytokines.^{12–15} In fact, the widespread release of inflammatory cytokines in severe COVID-19 patients may be sufficient to undermine the tight junctions of astrocytes and BBB endothelial cells, which facilitates the viral entry.^{16,17} Moreover, microglia and astrocytes are part of the local neuroinflammatory responses in the central nervous system (CNS). Thus, there are cellular receptors essential for the initiation or/and amplification of the innate immune responses of the CNS.^{18–22} Furthermore, the exposure to proinflammatory cytokines like IL-6, tumor necrosis factor alpha (TNF- α), IL-1 β , and reactive proinflammatory microglia as well as exposure to damage- and pathogen-associated molecular patterns may lead to the expression of proinflammatory genes in astrocytes, which is associated with neurodegeneration and neuroinflammation.^{21–24} Herein, we observed the increased expression of genes such as IL-1 β , IL-6, IFITM, MX1, and OAS2 in COVID-19 samples, suggesting the critical role of proinflammatory proteins (IL-1 β , IL-6) as well as interferon (IFN) responses marked by the upregulation of a subset of interferon-stimulated genes (IFITM, MX1, OAS2) in severe COVID-19 patients (Figure 6).

Spike glycoproteins of COVID-19 play an important role in viral binding to cellular receptors, particularly to the enzyme ACE2. Ubiquitous in the body, ACE2 plays a variety of physiological roles, including controlling inflammation and blood pressure. COVID-19 has a strong affinity with the ACE2 receptors. This receptor is present in neurons, endothelial cells, bronchial epithelial cells, and many other organs.^{25,26} It has been shown that ACE2 is expressed in a wide range of brain structures

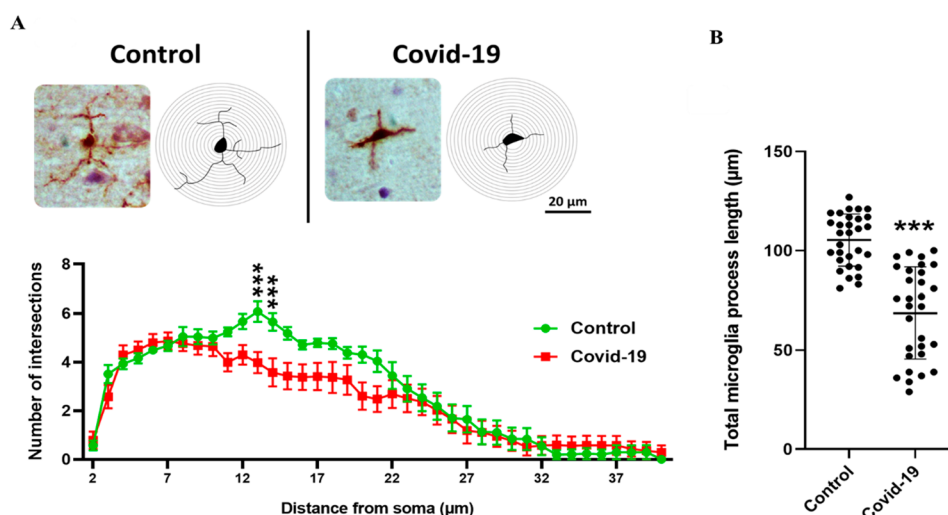


Figure 5. (A) Sholl analysis revealed a reduction in the microglial structural complexity with respect to long branching processes in the COVID-19 group. Moreover, (B) the total length of microglia processes was significantly reduced in the cerebral cortex of COVID-19 patients. (*) shows the difference between the control and COVID-19 group (*** $P < 0.001$).

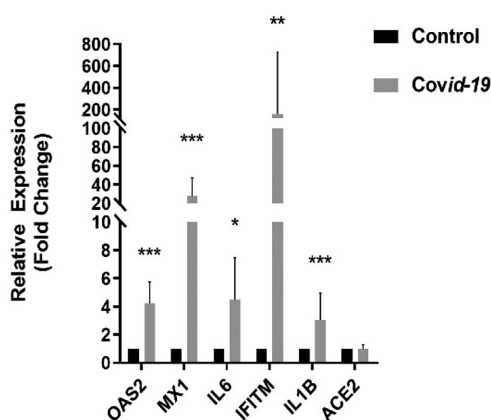


Figure 6. Expression levels of IL1B, MX1, OAS2 (*** $P < 0.001$), IFITM (** $P < 0.01$), and IL6 (* $P < 0.05$) were noticeably increased, while there was no significant difference in the expression level of ACE2. Beta actin (ACTB) is used as a housekeeping gene. The fold change for the control group was considered one for all genes, and the fold change for COVID-19 group was reported compared to that of the control.

including the hypothalamus, cortex, striatum, and brainstem.^{27–29} In addition, ACE2 is expressed in both neurons and glial cells throughout the brain, making both cell types vulnerable to the viruses.²⁹ In this regard, we measured the expression level of ACE2 using real time polymerase chain reaction (RT-PCR) in the human cerebral cortex region, but no significant difference was observed between COVID-19 and healthy groups (Figure 6). This is in line with a recent study that demonstrated very low or absence of ACE2 expression at transcript and protein levels in the human brain.³⁰

Recent studies have shown that COVID-19 patients with severe symptoms manifested lower glutathione (GSH) levels and higher reactive oxygen species (ROS).³¹ This demonstrates high ROS/GSH ratios in patients with critical conditions as opposed to those with mild symptoms. In fact, GSH acts as the main antioxidant in all tissues. The high concentration of its reduced forms highlights its major function in controlling different mechanisms such as immune response, protein folding,

antiviral defense, and detoxification.^{32,33} Therefore, the reduced GSH concentration in cells increases the viral replication cycle,^{34,35} which may be a possible cause of augmented COVID-19 infection in patients.³¹ In line with these studies, our results illustrated a significant decline in GSH level in the cerebral cortex of the COVID-19 group compared to that of the control (Figure 7). The GSH depletion in the alveolar fluid in patients

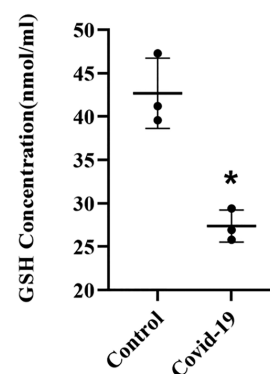


Figure 7. Graph shows a remarkable decrease in the level of GSH in COVID-19 patients as opposed to the controls (* $P < 0.05$).

with acute respiratory distress syndrome (ARDS) was found to be associated with enhanced ROS-mediated lung cell damage and inflammation.^{36,37} In fact, both a cytokine storm and ARDS have been known to be involved in severe stages of COVID-19.^{1,38} Similarly, the use of antioxidant agents can decrease the cytokine storm, which is caused by viral infection.³⁹ In fact, antioxidative-related treatments have been shown to repair damages caused by COVID-19 in infected patients.^{40,41} Polonikov et al. studied COVID-19 patients with moderate to severe symptoms, reporting that, while three cases with high or normal plasma GSH recovered expediently, one patient with low levels of GSH and high plasma levels of ROS and ROS/GSH ratio disclosed the most severe complications and was still sick until the publication of this paper.⁴² Overall, glia cells such as reactive astrocytes and activated microglia are able to produce free radicals, which could be neutralized by some antioxidant

enzymes like the GSH enzyme. Therefore, the decreased level of this enzyme in neurons can render neurons vulnerable to free radicals, ultimately leading to neuronal cell death.

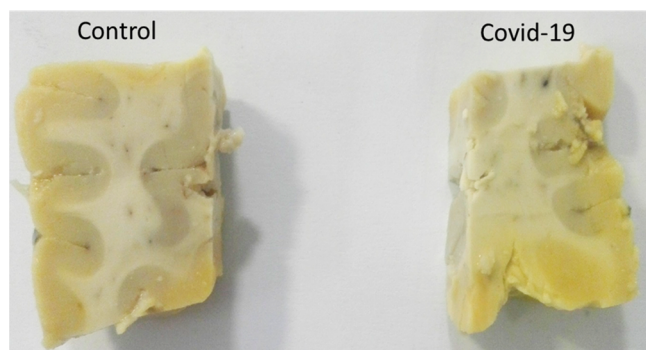


Figure S1. Supplementary Figure S1. Gross brain sections of control and COVID-19.

The major cause of mortality in COVID-19 patients is a cytokine storm, which is possibly caused by ROS.⁴³ It has also been shown that, in a seasonal influenza, the ROS level of the immune system decreases, and nicotinamide adenine dinucleotide phosphate (NADPH) oxidase-dependent bacterial clearance is suppressed. In viral infections, oxidative stress is associated with macrophage activation. In addition to the release of ROS, the activated phagocytes are also able to release pro-oxidant cytokines (e.g., TNF and IL-1), which can induce iron uptake in the reticuloendothelial system.⁴⁴ Similarly, viral infections not only can cause a neutrophil infiltration and ROS release but also can weaken the antioxidant defenses.⁴⁵ Therefore, it can be concluded that oxidative stress occurs because of an imbalance between the production of oxidants and antioxidant mechanisms, leading to oxidative damage (e.g., DNA oxidation and lipid peroxidation).

It has been shown that an increased level of IL-6 and a decreased level of GSH (in a positive feedback cycle) due to SARS-CoV infection can potentially elucidate the mechanism of a cytokine storm in this disease.⁴⁶ Likewise, a persistent GSH decrease is accompanied by an elevation of the levels of TGF, IL-6, and IL-10 in patients with human immunodeficiency virus (HIV).⁴⁷ This association was also confirmed by another study, in which they have found out that, following an administration of exogenous GSH (liposomal GSH), the level of these

inflammatory cytokines returned to normal.⁴⁸ Altogether, these reports might shed a light on the impact of ROS species on the antiviral and proinflammatory signaling in patients with severe COVID-19 infection.

Despite the prominent role of oxidative stress-mediated neuroinflammation in the neuronal death observed in patients with COVID-19, there are a host of limitations in this study that need to be properly addressed in future work. First, to strongly corroborate the findings, the number of subjects should be increased. Second, the levels of both oxidized and reduced forms of glutathione could be linked to other ROS/oxidative stress markers to evidently elucidate the role of oxidative stress and how it is related with neuroinflammatory response in the COVID-19 context. Third, to cast light on the infiltration of inflammatory cells, the quantification of other inflammatory cells such as brain pericytes, T cells, and mast cells needs to be conducted in severe COVID-19 patients.

In conclusion, our data suggest that glial-mediated neuroinflammation induced by oxidative stress plays a major role in the loss of neurons during a severe COVID-19 infection.

METHODS

Ethics and Informed Consent. The study was approved by the ethics committee of Shahid Beheshti University of Medical Sciences, Tehran, Iran (ethics committee No. IR.SBMU.RETE-CH.REC.1399.1118).

Sample and Data Collection. This study was conducted on three patients with COVID-19 and three age- and sex-matched healthy control groups. Control data were obtained from people in the age range of 20–40 years who met the following criteria: no history of neurological complications or addiction, dying of cardiac arrest or accident in which no head trauma was induced, and patients died of complications such as internal bleeding. The subjects were selected from among patients admitted to the intensive care unit (ICU) of a major university-affiliated hospital between March 26, 2020—the outbreak of the epidemic in Iran—and April 17, 2020. Three patients with clinical features including anosmia and respiratory symptoms compatible to COVID-19 were intubated due to respiratory distress. The diagnosis of COVID-19 was confirmed by RT-PCR. Additionally, a computed tomography (CT) scan showed pneumonia in the COVID-19 group. With a 30° rod telescope trough and an endoscopic transnasal approach, the cortex was harvested following the resection of the middle turbinate. In the control group, the brain tissues from three patients with myocardial infarction were included in this study.

Total RNA Isolation and cDNA Synthesis. The total RNA was successfully extracted from the brain tissues using RNX-Plus (SinaClon) according to the manufacturer's instructions. RNA

Table 2. Primer Sequences for qPCR

primer sequence	gene name	accession No.
F-CCCTGGACTTCGACAAGAG	<i>ACTB</i>	NM_001101
R-ACTCCATGCCAGGAAGAA		
F-GGGATCAGAGATCGGAAGAAGAAA	<i>ACE2</i>	NM_021804.3
R-AGGAGGTCTGAACATCATCAGTG		
F-AATCTGTACCTGTCCTGCGTGTT	<i>Il1b</i>	NM_000576.3
R-TGGGTAATTTTTGGGATCTACACTCT		
F-GGTACATCCTCGACGGCATCT	<i>Il6</i>	NM_001371096.1
R-GTGCCTCTTTGCTGCTTTTAC		
F-TGGCATAACCAGAGTGGCTG	<i>MX1</i>	NM_002462.5
R-CACCACCAGGCTGATTGTCT		
F-GCTTCCGACAATCAACAGCCAAG	<i>OAS2</i>	NM_016817.3
R-CTTGACGATTTTGTGCCGCTCG		
F-TCAACATCCACAGCGAGACC	<i>IFITM</i>	NM_003641.5
R-TGTACACAGAGCCGAATACCAG		

concentration, purity, and integrity were determined using an Epoch2 microplate reader (BioTeK) followed by the electrophoresis of the 5 μ L of extracted RNA in 2% agarose gels stained with ethidium bromide, which were visualized under a ultraviolet (UV) light. The cDNA from 500 ng of the total RNA isolated from the tissues was synthesized in 20 μ L of total volume using a RevertAid H Minus First Strand cDNA Synthesis Kit according to the manufacturer's instructions and then stored at -20 °C.

Quantitative Real Time PCR. Real-time quantitative PCR analysis was conducted using specific primers listed in Table 2 on a Rotor Gene6000 real-time PCR machine (Corbett Research, Qjagen). Beta actin (*ACTB*) was used as a housekeeping gene. Each reaction contained 1 μ L of the cDNA template, 0.4 μ L of each primer (20 pmole), and 10 μ L of SYBR Ampliqon, in the final volume of 20 μ L. The real-time PCR was performed in following steps. Stage 1: initial denaturation, 1 cycle at 95 °C for 90 s followed by stage 2: PCR, 40 cycles, each cycle lasting 95 °C for 15 s, 55 °C for 30 s. The comparative real-time qPCR quantitation was performed in candidate groups using the Relative Expression Software Tool (REST) 2009 (Qjagen).⁴⁹ The gene expression was reported as fold change compared with the control.

Estimating the Number of the Neuron and Glial Cells. The tissue samples were fixed in 10% formalin for one week. Then, tissues were embedded in paraffin blocks and cut into 20 μ m thick sections with a microtome. For the microscopic descriptive analysis of each group, slides were stained by H&E. The optical disector method was used to determine the total numbers of the neuron and glial cells. Moreover, an unbiased counting frame containing the exclusion and inclusion boundaries was superimposed on the images of sections observed on the monitor. The focal plane moved down in the Z direction, and a microcator was connected to the microscope stage to measure the z-axis motion. Each nucleus of neurons and glial cells coming into maximal focus was selected if it was within the counting frame. The following formula was used to calculate the numerical density (N_v): $N_v = \frac{\sum Q}{\sum P \times h \times \frac{a}{f}} \times \frac{t}{BA}$. Here, $\sum Q$ indicates the number of nuclei, h is the disector height, a/f is the frame area, and $\sum P$ indicates total numbers of the unbiased counting frame in each field. Moreover, t denotes the real thickness of the section gauged in all fields with a microcator. In addition, BA stands for the microtome block advance.⁵⁰

The Measurement of Spatial Distribution of Neurons. The spatial distribution of neurons in the cerebral cortex was measured by a Voronoi tessellation method. The cerebral cortex neurons were mapped by the ImageJ Voronoi Plugin (Java. NIH). Each polygon was drawn around the cell body of neurons. In this regard, brain sections images were captured by 40 \times objective lens (Nikon Eclipse E-200). Then, each image was imported to ImageJ, and the polygons were drawn by clicking on the nuclei, followed by the assessment of the polygon area and coefficient of variation. CV values of 33%–64% are associated with a random distribution of the neurons; CVs less than 33% indicate a regular pattern, and those more than 64% are considered as a clustered distribution.⁵¹

Immunohistochemistry. Brain tissues were placed in formalin before being prepared and placed on the slides. The primary antibodies against GFAP (ABCAM, catalogue No. ab7260, 1:300) and Iba-1 (ABCAM, catalogue No. ab108539, 1:300) were diluted in the phosphate-buffered saline (PBS) solution containing 0.3% Triton X-100 and 1% bovine serum albumin (BSA). After the slide preparation, sections were incubated in primary antibodies overnight at 4 °C. They were then incubated with the avidin–biotin complex substrate in the milieu of the 0.05 M Tris-buffer (pH 7.6) containing 0.05% 3,3-diaminobenzidine tetrahydrochloride and 0.03% hydrogen peroxide. Finally, sections were mounted and counter-stained followed by the implementation of the optical disector method to determine the total numbers of microglia and astrocytes. The results were reported as a numerical density (number/mm³).

The Assessment of Microglia Morphology by a Sholl Analysis. To specifically detect microglial cells, the cells were labeled with Iba-1 antibody (a microglia-specific marker). The microscopic images were captured by a 40 \times objective lens (Nikon Eclipse E-200).

Thirty individual microglial cells per patient were selected for the reconstruction and also for the measurement of the length of microglia processes using ImageJ (Java. NIH).⁵²

Measurement of GSH Content. When they were received, the brain tissues (the cerebral cortex) were stored at -80 °C. On the day of sample preparation, brain tissues were removed from the -80 °C storage and thawed in the PBS lysis buffer (pH 7.4) containing 320 mM sucrose, 1% of 1.0 M Tris-HCl (pH = 8.8), 0.098 mM of MgCl₂, 0.076 mM of ethylenediaminetetraacetic acid (EDTA), and the phosphatase inhibitor cocktail (Sigma-Aldrich). The brain tissues were homogenized by 10 quick pulses using a hand-held homogenizer. The homogenates were centrifuged at 14 000g for 10 min to remove cellular debris. GSH reacts with 5,5-dithiobis (2-nitrobenzoic acid) (DTNB) to form the colored product 2-nitro-5-thiobenzoic acid, which was estimated at 412 nm.⁵³

Statistical Analyses. All statistical analyses were performed using SPSS 23.0 (SPSS, Inc.). Data are presented as mean \pm standard deviation (SD). Differences between experimental groups were investigated by the independent sample *t*-test. *P* values less than 0.05 were considered as significant.

AUTHOR INFORMATION

Corresponding Authors

Abbas Aliaghaei – Brain Mapping Research Center and Department of Cell Biology and Anatomical Sciences, School of Medicine, Shahid Beheshti University of Medical Sciences, Tehran 19857-17443, Iran; orcid.org/0000-0003-4668-5175; Phone: +982123872577; Email: aghaei60@gmail.com

Mohammad-Amin Abdollahifar – Brain Mapping Research Center and Department of Cell Biology and Anatomical Sciences, School of Medicine, Shahid Beheshti University of Medical Sciences, Tehran 19857-17443, Iran; orcid.org/0000-0001-6947-3285; Phone: +982122439976; Email: abdollahima@sbmu.ac.ir

Authors

Mahdi Eskandarian Boroujeni – Laboratory of Human Molecular Genetics, Institute of Molecular Biology and Biotechnology, Faculty of Biology, Adam Mickiewicz University, Poznan 61-614, Poland

Leila Simani – Skull Base Research Center, Loghman Hakim Hospital, Shahid Beheshti University of Medical Sciences, Tehran 1333635445, Iran; orcid.org/0000-0002-1349-4252

Hans A. R. Bluysen – Laboratory of Human Molecular Genetics, Institute of Molecular Biology and Biotechnology, Faculty of Biology, Adam Mickiewicz University, Poznan 61-614, Poland

Hamid Reza Samadikhah – Department of Biology, Faculty of Sciences, Central Tehran Branch, Islamic Azad University, Tehran 13185/768, Iran

Soheila Zamanlui Benisi – Stem Cell Research Center, Tissue Engineering and Regenerative Medicine Institute, Central Tehran Branch, Islamic Azad University, Tehran 13185/768, Iran

Sanaz Hassani – Laboratory of Human Molecular Genetics, Institute of Molecular Biology and Biotechnology, Faculty of Biology, Adam Mickiewicz University, Poznan 61-614, Poland

Nader Akbari Dilmaghani – Skull Base Research Center, Loghman Hakim Hospital, Shahid Beheshti University of Medical Sciences, Tehran 1333635445, Iran

Mobina Fathi – Student Research Committee, Faculty of Medicine, Shahid Beheshti University of Medical Sciences, Tehran 19857-17443, Iran

Kimia Vakili – Student Research Committee, Faculty of Medicine, Shahid Beheshti University of Medical Sciences, Tehran 19857-17443, Iran

Gholam-Reza Mahmoudiasl – Legal Medicine Organization, Legal Medicine Research Center, Tehran 1114795113, Iran; Laser Application in Medical Sciences Research Center, Shahid Beheshti University of Medical Sciences, Tehran 19857-17443, Iran

Hojjat Allah Abbaszadeh – Laser Application in Medical Sciences Research Center and Department of Cell Biology and Anatomical Sciences, School of Medicine, Shahid Beheshti University of Medical Sciences, Tehran 19857-17443, Iran

Meysam Hassani Moghaddam – Department of Anatomical Sciences, School of Medicine, Shiraz University of Medical Sciences, Shiraz 71348-14336, Iran

Complete contact information is available at:

<https://pubs.acs.org/10.1021/acscchemneuro.1c00111>

Author Contributions

●(M.E.B. and L.S.) These authors contributed equally to this work. H.R.S., S.Z.B., N.A.D., M.F., K.V., G.R.M., H.A.A., and M.H.M. had a role in the acquisition of data. M.E.B. and A.A. conceptualized it and drafted the manuscript for intellectual content. L.S., A.A., and M.A.A. designed and conceived the study. S.H. and H.A.A. analyzed and interpreted the data, and H.A.R.B. and M.E.B. revised the manuscript.

Funding

This research received no specific grant from any funding agency in the public, commercial, or not-for-profit sectors.

Notes

The authors declare no competing financial interest.

ACKNOWLEDGMENTS

The authors thank all the officials and staff in Clinical Research Development Unit (CRDU) of Loghman Hakim Hospital, Shahid Beheshti University of Medical Sciences, Tehran, Iran, for their enormous and collaborative efforts in this project. We also appreciate the Iranian Legal Medicine organization for giving us the opportunity to have access to the patient registries and biological samples.

ABBREVIATIONS

COVID-19; coronavirus disease 19; GSH; glutathione; CSF; cerebrospinal fluid; BBB; blood–brain barrier; CNS; central nervous system; CV; coefficient of variation; IL-1 β ; interleukin 1 beta; TNF- α ; tumor necrosis factor alpha; IFITM; interferon-inducible transmembrane, MX1, MX dynamin-like GTPase 1; OAS2; 2',5'-oligoadenylate synthetase 2; IL-6; interleukin 6; ROS; reactive oxygen species.

REFERENCES

- (1) Sestili, P., and Fimognari, C. (2020) Paracetamol-Induced Glutathione Consumption: Is There a Link With Severe COVID-19 Illness? *Front. Pharmacol.* *11*, 1597.
- (2) Khatoun, F., Prasad, K., and Kumar, V. (2020) Neurological manifestations of COVID-19: available evidences and a new paradigm. *J. NeuroVirol.* *26*, 619.
- (3) Wang, H.-Y., Li, X.-L., Yan, Z.-R., Sun, X.-P., Han, J., and Zhang, B.-W. (2020) Potential neurological symptoms of COVID-19. *Therapeutic Advances in Neurological Disorders* *13*, 175628642091783.
- (4) Rhea, E. M., Logsdon, A. F., Hansen, K. M., Williams, L. M., Reed, M. J., Baumann, K. K., Holden, S. J., Raber, J., Banks, W. A., and

Erickson, M. A. (2021) The S1 protein of SARS-CoV-2 crosses the blood–brain barrier in mice. *Nat. Neurosci.* *24*, 368.

(5) Lucchese, G. (2020) Cerebrospinal fluid findings in COVID-19 indicate autoimmunity. *Lancet Microbe* *1*, e242.

(6) Lee, M.-H., Perl, D. P., Nair, G., Li, W., Maric, D., Murray, H., Dodd, S. J., Koretsky, A. P., Watts, J. A., and Cheung, V. (2021) Microvascular Injury in the Brains of Patients with Covid-19. *N. Engl. J. Med.* *384*, 481.

(7) Tremblay, M.-E., Madore, C., Bordeleau, M., Tian, L., and Verkhratsky, A. (2020) Neuropathobiology of COVID-19: the role for glia. *Front. Cell. Neurosci.* *14*. DOI: 10.3389/fncel.2020.592214

(8) Kanberg, N., Ashton, N. J., Andersson, L.-M., Yilmaz, A., Lindh, M., Nilsson, S., Price, R. W., Blennow, K., Zetterberg, H., and Gisslén, M. (2020) Neurochemical evidence of astrocytic and neuronal injury commonly found in COVID-19. *Neurology* *95*, e1754–e1759.

(9) Reichard, R. R., Kashani, K. B., Boire, N. A., Constantopoulos, E., Guo, Y., and Lucchinetti, C. F. (2020) Neuropathology of COVID-19: a spectrum of vascular and acute disseminated encephalomyelitis (ADEM)-like pathology. *Acta Neuropathol.* *140*, 1–6.

(10) Yang, R., Wang, H., Wen, J., Ma, K., Chen, D., Chen, Z., and Huang, C. (2019) Regulation of microglial process elongation, a featured characteristic of microglial plasticity. *Pharmacol. Res.* *139*, 286–297.

(11) Palpagama, T. H., Waldvogel, H. J., Faull, R. L., and Kwakowsky, A. (2019) The role of microglia and astrocytes in Huntington's disease. *Front. Mol. Neurosci.* *12*, 258.

(12) Perry, V. H., Cunningham, C., and Holmes, C. (2007) Systemic infections and inflammation affect chronic neurodegeneration. *Nat. Rev. Immunol.* *7*, 161–167.

(13) Teeling, J., and Perry, V. (2009) Systemic infection and inflammation in acute CNS injury and chronic neurodegeneration: underlying mechanisms. *Neuroscience* *158*, 1062–1073.

(14) Murta, V., and Ferrari, C. (2016) Peripheral inflammation and demyelinating diseases. In *Glial Cells in Health and Disease of the CNS* pp 263–285, Springer.

(15) Yamout, B., Hourani, R., Salti, H., Barada, W., El-Hajj, T., Al-Kutoubi, A., Herlopian, A., Baz, E. K., Mahfouz, R., Khalil-Hamdan, R., et al. (2010) Bone marrow mesenchymal stem cell transplantation in patients with multiple sclerosis: a pilot study. *J. Neuroimmunol.* *227*, 185–189.

(16) Li, F., Wang, Y., Yu, L., Cao, S., Wang, K., Yuan, J., Wang, C., Wang, K., Cui, M., and Fu, Z. F. (2015) Viral infection of the central nervous system and neuroinflammation precede blood-brain barrier disruption during Japanese encephalitis virus infection. *J. Virol.* *89*, 5602–5614.

(17) Swanson, P. A., and McGavern, D. B. (2015) II, McGavern DB. Viral diseases of the central nervous system. *Curr. Opin. Virol.* *11*, 44–54.

(18) Farina, C., Aloisi, F., and Meinl, E. (2007) Astrocytes are active players in cerebral innate immunity. *Trends Immunol.* *28*, 138–145.

(19) Russo, M. V., and McGavern, D. B. (2015) Immune surveillance of the CNS following infection and injury. *Trends Immunol.* *36*, 637–650.

(20) Hwang, M., and Bergmann, C. C. (2018) Alpha/Beta interferon (IFN- α/β) signaling in astrocytes mediates protection against viral encephalomyelitis and regulates IFN- γ -dependent responses. *J. Virol.* *92*. DOI: 10.1128/JVI.01901-17

(21) Rosciszewski, G., Cadena, V., Murta, V., Lukin, J., Villarreal, A., Roger, T., and Ramos, A. J. (2017) Toll-like receptor 4 (TLR4) and triggering receptor expressed on myeloid cells-2 (TREM-2) activation balance astrocyte polarization into a proinflammatory phenotype. *Mol. Neurobiol.* *55*, 3875–3888.

(22) Rosciszewski, G. A., Cadena, V., Auzmendi, J. A., Cieri, M. B., Lukin, J., Rossi, A. R., Murta, V., Villarreal, A., Reines, A., Gomes, F., et al. (2019) Detrimental effects of HMGB-1 require microglial-astroglial interaction: implications for the status epilepticus-induced neuroinflammation. *Front. Cell. Neurosci.* *13*, 380.

(23) Liddelow, S. A., and Barres, B. A. (2017) Reactive astrocytes: production, function, and therapeutic potential. *Immunity* *46*, 957–967.

- (24) Liddelow, S. A., Guttenplan, K. A., Clarke, L. E., Bennett, F. C., Bohlen, C. J., Schirmer, L., Bennett, M. L., Münch, A. E., Chung, W.-S., Peterson, T. C., et al. (2017) Neurotoxic reactive astrocytes are induced by activated microglia. *Nature* 541, 481–487.
- (25) Gupta, A., Madhavan, M. V., Sehgal, K., Nair, N., Mahajan, S., Sehrawat, T. S., Bikdeli, B., Ahluwalia, N., Ausiello, J. C., Wan, E. Y., et al. (2020) Extrapulmonary manifestations of COVID-19. *Nat. Med.* 26, 1017–1032.
- (26) Shang, J., Wan, Y., Luo, C., Ye, G., Geng, Q., Auerbach, A., and Li, F. (2020) Cell entry mechanisms of SARS-CoV-2. *Proc. Natl. Acad. Sci. U. S. A.* 117, 11727–11734.
- (27) Forward, D. F. (2020) User menu, *In Vitro*.
- (28) Xia, H., and Lazartigues, E. (2008) Angiotensin-converting enzyme 2 in the brain: properties and future directions. *J. Neurochem.* 107, 1482–1494.
- (29) Baig, A. M., Khaleeq, A., Ali, U., and Syeda, H. (2020) Evidence of the COVID-19 virus targeting the CNS: tissue distribution, host–virus interaction, and proposed neurotropic mechanisms. *ACS Chem. Neurosci.* 11, 995–998.
- (30) Hikmet, F., Méar, L., Edvinsson, Å., Micke, P., Uhlén, M., and Lindskog, C. (2020) The protein expression profile of ACE2 in human tissues. *Mol. Syst. Biol.* 16, e9610.
- (31) Jaiswal, N., Bhatnagar, M., and Shah, H. (2020) N-acetylcysteine: A potential therapeutic agent in COVID-19 infection. *Med. Hypotheses* 144, 110133.
- (32) Forman, H. J., Zhang, H., and Rinna, A. (2009) Glutathione: overview of its protective roles, measurement, and biosynthesis. *Mol. Aspects Med.* 30, 1–12.
- (33) Silvagno, F., Vernone, A., and Pescarmona, G. P. (2020) The role of glutathione in protecting against the severe inflammatory response triggered by COVID-19. *Antioxidants* 9, 624.
- (34) Amatore, D., Sgarbanti, R., Aquilano, K., Baldelli, S., Limongi, D., Civitelli, L., Nencioni, L., Garaci, E., Ciriolo, M. R., and Palamara, A. T. (2015) Influenza virus replication in lung epithelial cells depends on redox-sensitive pathways activated by NOX4-derived ROS. *Cell. Microbiol.* 17, 131–145.
- (35) Fraternali, A., Paoletti, M. F., Casabianca, A., Nencioni, L., Garaci, E., Palamara, A. T., and Magnani, M. (2009) GSH and analogs in antiviral therapy. *Mol. Aspects Med.* 30, 99–110.
- (36) Pacht, E. R., Timerman, A. P., Lykens, M. G., and Merola, J. (1991) Deficiency of alveolar fluid glutathione in patients with sepsis and the adult respiratory distress syndrome. *Chest* 100, 1397–1403.
- (37) Sadegh Soltan-Sharifi, M., Mojtahedzadeh, M., Najafi, A., Reza Khajavi, M., Reza Rouini, M., Moradi, M., Mohammadirad, A., and Abdollahi, M. (2007) Improvement by N-acetylcysteine of acute respiratory distress syndrome through increasing intracellular glutathione, and extracellular thiol molecules and anti-oxidant power: evidence for underlying toxicological mechanisms. *Hum. Exp. Toxicol.* 26, 697–703.
- (38) Soy, M., Keser, G., Atagündüz, P., Tabak, F., Atagündüz, I., and Kayhan, S. (2020) Cytokine storm in COVID-19: pathogenesis and overview of anti-inflammatory agents used in treatment. *Clin. Rheumatol.* 39, 2085.
- (39) Luo, P., Liu, D., and Li, J. (2020) Pharmacologic perspective: glycyrrhizin may be an efficacious therapeutic agent for COVID-19. *Int. J. Antimicrob. Agents* 55, 105995.
- (40) Wang, J.-Z., Zhang, R.-Y., and Bai, J. (2020) An anti-oxidative therapy for ameliorating cardiac injuries of critically ill COVID-19-infected patients. *Int. J. Cardiol.* 312, 137.
- (41) Zabetakis, I., Lordan, R., Norton, C., and Tsoupras, A. (2020) COVID-19: The Inflammation Link and the Role of Nutrition in Potential Mitigation. *Nutrients* 12, 1466.
- (42) Polonikov, A. (2020) Endogenous Deficiency of Glutathione as the Most Likely Cause of Serious Manifestations and Death in COVID-19 Patients. *ACS Infect. Dis.* 6, 1558.
- (43) Dai, X., and Ostrikov, K. K. (2021) ROS-Driven selection pressure on COVID-19 patients with cardiovascular comorbidities. *Innovation*, 100107.
- (44) Sun, K., and Metzger, D. W. (2014) Influenza infection suppresses NADPH oxidase–dependent phagocytic bacterial clearance and enhances susceptibility to secondary methicillin-resistant *Staphylococcus aureus* infection. *J. Immunol.* 192, 3301–3307.
- (45) Laforge, M., Elbim, C., Frère, C., Hémadi, M., Massaad, C., Nuss, P., Benoliel, J.-J., and Becker, C. (2020) Tissue damage from neutrophil-induced oxidative stress in COVID-19. *Nat. Rev. Immunol.* 20, 515–516.
- (46) LIAO, Q. J., YE, L. B., Timani, K. A., ZENG, Y. C., SHE, Y. L., Ye, L., and WU, Z. H. (2005) Activation of NF- κ B by the full-length nucleocapsid protein of the SARS coronavirus. *Acta Biochim. Biophys. Sin.* 37, 607–612.
- (47) Ly, J., Lagman, M., Saing, T., Singh, M. K., Tudela, E. V., Morris, D., Anderson, J., Daliva, J., Ochoa, C., Patel, N., et al. (2015) Liposomal glutathione supplementation restores TH1 cytokine response to Mycobacterium tuberculosis infection in HIV-infected individuals. *J. Interferon Cytokine Res.* 35, 875–887.
- (48) Valdivia, A., Ly, J., Gonzalez, L., Hussain, P., Saing, T., Islamoglu, H., Pearce, D., Ochoa, C., and Venketaraman, V. (2017) Restoring cytokine balance in HIV-positive individuals with low CD4 T cell counts. *AIDS Res. Hum. Retroviruses* 33, 905–918.
- (49) Pfaffl, M. W., Horgan, G. W., and Dempfle, L. (2002) Relative expression software tool (REST[®]) for group-wise comparison and statistical analysis of relative expression results in real-time PCR. *Nucleic Acids Res.* 30, 36e.
- (50) Aghajanianpour, F., Boroujeni, M. E., Jahanian, A., Soltani, R., Ezi, S., Khatmi, A., Abdollahifar, M. A., Mirbehbahani, S. H., Toreyhi, H., Aliaghaei, A., and Amini, A. (2020) Tramadol: a Potential Neurotoxic Agent Affecting Prefrontal Cortices in Adult Male Rats and PC-12 Cell Line. *Neurotoxic. Res.* 38, 385–397.
- (51) Duyckaerts, C., and Godefroy, G. (2000) Voronoi tessellation to study the numerical density and the spatial distribution of neurones. *J. Chem. Neuroanat.* 20, 83–92.
- (52) Kongsui, R., Beynon, S. B., Johnson, S. J., and Walker, F. R. (2014) Quantitative assessment of microglial morphology and density reveals remarkable consistency in the distribution and morphology of cells within the healthy prefrontal cortex of the rat. *J. Neuroinflammation* 11, 1–9.
- (53) Ellman, G. L. (1959) Tissue sulfhydryl groups. *Arch. Biochem. Biophys.* 82, 70–77.